

This is a repository copy of *Interocular interaction of contrast and luminance signals in human primary visual cortex*.

White Rose Research Online URL for this paper:

<https://eprints.whiterose.ac.uk/id/eprint/123813/>

Version: Accepted Version

---

**Article:**

Chadnova, Eva, Reynaud, Alexandre, Clavagnier, Simon et al. (3 more authors) (2018) Interocular interaction of contrast and luminance signals in human primary visual cortex. *Neuroimage*. 23 - 30. ISSN 1053-8119

<https://doi.org/10.1016/j.neuroimage.2017.10.035>

---

**Reuse**

This article is distributed under the terms of the Creative Commons Attribution-NonCommercial-NoDerivs (CC BY-NC-ND) licence. This licence only allows you to download this work and share it with others as long as you credit the authors, but you can't change the article in any way or use it commercially. More information and the full terms of the licence here: <https://creativecommons.org/licenses/>

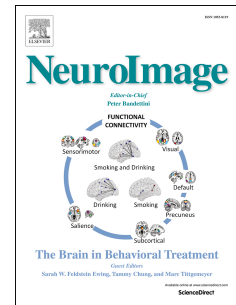
**Takedown**

If you consider content in White Rose Research Online to be in breach of UK law, please notify us by emailing [eprints@whiterose.ac.uk](mailto:eprints@whiterose.ac.uk) including the URL of the record and the reason for the withdrawal request.

# Accepted Manuscript

Interocular interaction of contrast and luminance signals in human primary visual cortex

E. Chadnova, A. Reynaud, S. Clavagnier, D.H. Baker, S. Baillet, R.F. Hess



PII: S1053-8119(17)30862-5

DOI: [10.1016/j.neuroimage.2017.10.035](https://doi.org/10.1016/j.neuroimage.2017.10.035)

Reference: YNIMG 14413

To appear in: *NeuroImage*

Received Date: 1 February 2017

Revised Date: 11 October 2017

Accepted Date: 17 October 2017

Please cite this article as: Chadnova, E., Reynaud, A., Clavagnier, S., Baker, D.H., Baillet, S., Hess, R.F., Interocular interaction of contrast and luminance signals in human primary visual cortex, *NeuroImage* (2017), doi: 10.1016/j.neuroimage.2017.10.035.

This is a PDF file of an unedited manuscript that has been accepted for publication. As a service to our customers we are providing this early version of the manuscript. The manuscript will undergo copyediting, typesetting, and review of the resulting proof before it is published in its final form. Please note that during the production process errors may be discovered which could affect the content, and all legal disclaimers that apply to the journal pertain.

# Interocular interaction of contrast and luminance signals in human primary visual cortex

Chadnova, E.<sup>1</sup>, Reynaud, A.<sup>1</sup>, Clavagnier, S.<sup>1</sup>, Baker, D.H.<sup>2</sup>, Baillet, S.<sup>3\*</sup>, and Hess, R. F.<sup>1\*</sup>

<sup>1</sup> McGill Vision Research, Dept. Ophthalmology, McGill University,

<sup>2</sup> Dept. Psychology, University of York, UK

<sup>3</sup> McConnell Brain Imaging Centre, Montreal Neurological Institute, McGill University, Montreal, QC  
Canada

\*correspondence to: robert.hess@mcgill.ca

sylvain.baillet@mcgill.ca

## 1. Abstract

Interocular interaction in the visual system occurs under dichoptic conditions when contrast and luminance are imbalanced between the eyes. Human psychophysical investigations suggest that interocular interaction can be explained by a contrast normalization model. However, the neural processes that underlie such interactions are still unresolved. We set out to assess, for the first time, the proposed normalization model of interocular contrast interactions using magnetoencephalography and to extend this model to incorporate interactions based on interocular luminance differences. We used magnetoencephalography to record steady-state visual evoked responses (SSVER), and functional magnetic resonance imaging (fMRI) to obtain individual retinotopic maps that we used in combination with MEG source imaging in healthy participants. Binary noise stimuli were presented in monocular or dichoptic viewing and were frequency-tagged at 4 and 6 Hz. The contrast of the stimuli was modulated in a range between 0 to 32%. Monocularly, we reduced the luminance by placing a 1.5 ND filter over one eye in the maximal contrast condition. This ND filter reduces the mean light level by a factor of 30 without any alteration to the physical contrast.

We observed in visual area V1 a monotonic increase in the magnitude of SSVERs with changes in contrast from 0 to 32%. For both eyes, dichoptic masking induced a decrease in SSVER signal power. This power decrease was well explained by the normalization model. Reducing mean luminance delayed monocular processing by approximately 38 ms in V1. The reduced luminance also decreased the masking ability of the eye under the filter. Predictions based on a temporal filtering model for the interocular luminance difference prior to the model's binocular combination stage were incorporated to update the normalization model. Our results demonstrate that the signals resulting from different contrast or luminance stimulation of the two eyes are combined in a way that can be explained by an interocular normalization model.

## 2. Introduction

Visual neurons have a limited dynamic range. To ensure the optimal transduction of contrast signals there is a need to ensure that the responsiveness is set about the prevailing contrast conditions. This is achieved by a normalization (Heeger 1991; Carandini and Heeger, 1994) where the contrast response of a particular neuron is divided by the sum of the contrast responses of neighboring neurons. One consequence of this behavior is that the response to a stimulus is reduced by the presence of another overlaid stimulus, referred to as masking. These effects have been well documented in the human psychophysics literature (Legge and Foley, 1980; Foley 1994) and in many studies of the animal visual system (Cavanaugh et al., 2002). They are also well described by gain control models (Carandini and Heeger, 1994; Busse et al., 2009; Reynaud et al., 2012). Human electrophysiological studies have further developed our understanding of monocular masking as a result of signal normalization and provided insights into its dynamics (Tsai et al., 2012). A similar issue is involved with the combination of left and right eye contrast responses and there is a psychophysical literature on normalization models to describe it (Legge 1984, Ding and Sperling, 2006, Meese et al., 2006). Evidence from functional magnetic resonance imaging (fMRI) data suggests a type of normalization in which the signals from each eye contribute to a normalization of both eyes, so called interocular normalization (Moradi and Heeger, 2009).

In this work, we further examined how the contrast responses between the two eyes interact and how this interaction is altered when one eye is exposed to a different mean luminance, a condition that we argue alters the temporal filtering properties of the visual system (Reynaud et al., 2013). We use a novel steady-state visually evoked response (SSVER) magnetoencephalography protocol combined with a time-resolved

neuroimaging approach. This MEG approach uniquely identifies left and right-eye signals (Norcia et al., 2015) and allows an independent examination of the important issue of how signals are combined between the two eyes.

We addressed the following key questions regarding binocular processing: 1. Can dichoptic interactions be assessed with MEG and if so, do current interocular normalization models (Ding and Sperling, 2006; Meese et al., 2006; Moradi and Heeger, 2009) provide adequate prediction of such interactions at various contrasts of target and mask? 2. How does the effect of interocular differences in luminance compare to that of interocular differences in contrast at monocular and dichoptic levels, and can this be incorporated into a interocular normalization model? To the best of our knowledge, no previous study has addressed this issue.

### 3. Methods

#### 3.1 Participants

Five male participants (mean age 31.4 +/- 4.9 years) volunteered for the contrast modulation experiment. Seven participants (1 female, mean age: 29.7 +/- 6 years old) took part in the luminance modulation study. All had normal vision. All participants provided signed informed consent following the procedure approved by the Research Ethics Board of the Montreal Neurological Institute, consistent with the Declaration of Helsinki. One volunteer was later excluded from the luminance modulation study due to head movement artifacts in the collected data; full data analysis was therefore performed on six subjects for that experiment.

### 3.2 Stimuli

The experimental presentation was coded in the Psychophysics toolbox (Brainard, 1997; Pelli, 1997) in Matlab. Before running the current experiment, we performed a pilot study on one of our participants aiming to select the best stimulus to demonstrate monocular response as well as the masking ability at various contrast levels. The results of that pilot investigation are presented in Supplementary Figure 1. Based on the obtained results, we selected our stimulus to be a checkerboard pattern of binary noise with a box size of 10 pixels that translated into 0.1 degrees of visual angle (Figure 1a). The contrast calculations were expressed as Michelson contrast units expressed as a percentage. The visual stimuli were presented dichoptically; the contrast to each eye could be varied independently. The steady-state visually evoked response paradigm was adapted from Norcia et al. (2015) with a temporally contrast modulated stimulus (onset/offset mode) at frequencies of 4 Hz and 6 Hz (Figure 1A). The stimuli occupied 8 degrees in the visual field. The trial duration was 4 seconds, with a 1.5-second inter-trial interval. A fixation cross was placed at the center of the visual field at all times. We used a 60-Hz refresh rate gamma-corrected passive 3D LCD LG D2342P monitor (23'', 1920 X 1080, active area 509 X 290 mm). The monitor was viewed with polarized glasses to enable dichoptic stimulation, hence odd and even scan lines were displayed to each eye and blocked to the other eye respectively. This induced a decrease to about 40% of the initial monitor luminance, resulting in a viewed mean luminance of 47 cd/m<sup>2</sup> through the polarizers. The screen was placed 170 cm from the observer in a dark magnetically shielded MEG room.

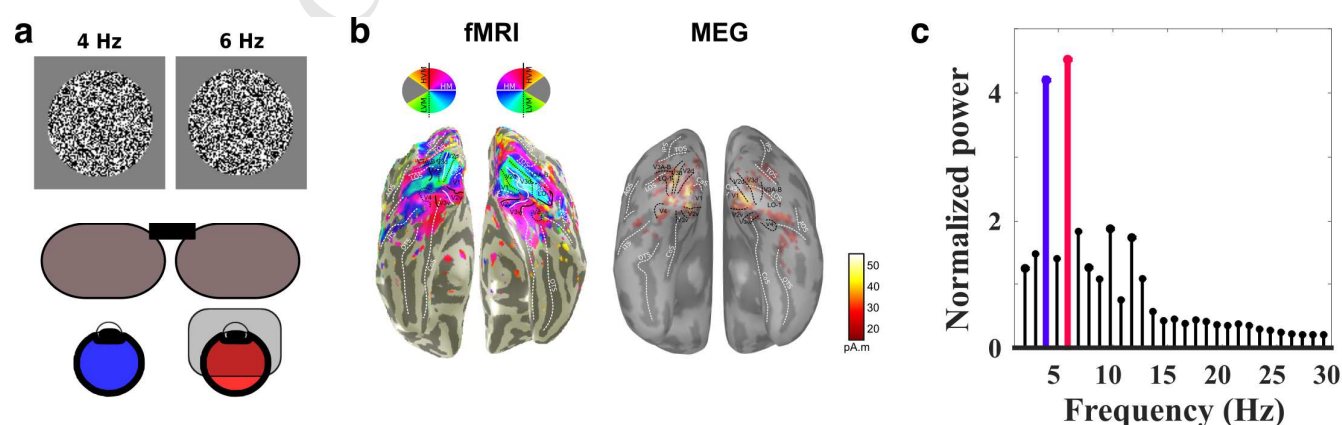


**Figure1. Illustrations of experimental setup and methods.**

- a. Binary noise pattern was projected at flicker frequencies of 4 and 6 Hz to non-dominant and dominant eyes accordingly. The stimulus was shown on a 3D LG monitor and viewed through a pair of LG polarizers. During the reduced luminance trials, a 1.5 ND filter was applied to the dominant eye (6 Hz eye).
- b. The regions of interests (left and right V1) were extracted from individually obtained fMRI retinotopy maps.
- c. Sample power spectrum density of the response to the dichoptic stimulation in V1. The fundamental frequencies are shown in color (4 Hz in blue and 6Hz in red).

### 3.3 Procedure

Data collection consisted of two sessions, recorded separately: Session 1 followed a contrast variation protocol with a fixed mean luminance; Session 2 consisted of a luminance variation protocol with fixed contrast.

The contrast modulation experiment (Session 1) consisted of five blocks of trials, each comprising 10 repetitions of each of 10 tested conditions. The 10 different conditions consisted of 5 contrasts (0%, 4%, 8%, 16% and 32%) presented monocularly (i.e. with 0% contrast mean gray shown to the other eye) and under the dichoptic mask of 32% contrast. The fixed contrast mask was projected to the dominant eye (left eye for 3 participants) and was tagged at 6Hz, whereas the stimulus with a condition-dependent contrast was tagged at 4Hz. The condition with 0% contrast in both eyes (blank condition) was later used for normalizing the data for each participant.

The luminance modulation experiment (Session 2) consisted of six trial blocks: 3 with normal luminance and 3 with monocularly reduced luminance. The blocks were randomly interleaved between participants and lasted 10 minutes each. Luminance reduction was achieved by placing a 1.5 ND filter in front of the right eye. The stimulus to the right eye was tagged at 6Hz. Each block included 20 repetitions of 4



conditions tested: 0% contrast to both eyes (blank), 32% contrast in the right eye (monocular right), 32% contrast in the left eye (monocular left), 32% contrast in both eyes (dichoptic) randomly ordered, for a total of 60 repetitions for each condition. Subjects were instructed to maintain fixation, looking at a central crosshair.

### 3.4 MEG data acquisition

All recordings started with a 2-minute MEG noise recording, to capture daily environmental noise statistics (sample data covariance across MEG channels) that were later used for MEG source modeling.

MEG data were collected using a CTF OMEGA System with 275 axial gradiometers, inside a 3-layer magnetically shielded room. A Polhemus Isotrak system was used to digitize the participants' fiducial landmarks (nasion and pre-auricular points) and head shape, using approximately 60 face and scalp points. Three head position indicator coils were fixed to the participants' head and referenced to the other digitized landmarks, to localize the head's position with the MEG system at the beginning of each block. Two EOG electrodes aimed at recording the eye blinks and saccades were placed above and below the left eye. Two electrodes were placed across the plane of the chest to collect electrocardiographic (ECG) signals. Data were initially sampled at 2.4 kHz.

### 3.5 Individual retinotopic atlas from fMRI

MEG source analyses were constrained to each participant's anatomy and retinotopically (functionally) defined regions of interest (ROIs). These ROIs were obtained from fMRI data of the same participants for other studies (Figure 1b, Clavagnier et al., 2015). Volume segmentation of structural T1 MRI was performed with Freesurfer (<http://surfer.nmr.mgh.harvard.edu/>). We used the methods described in Dumoulin and Wandell (2008) and Clavagnier et al. (2015) to derive the population receptive fields from our fMRI data. This analysis was performed in mrVista ([http://white.stanford.edu/newlm/index.php/Main\\_Page](http://white.stanford.edu/newlm/index.php/Main_Page)). The borders of cortical visual area V1 were identified for every subject based on the location of the visual meridians (Engel et al., 1994). This region

(V1) was imported into FreeSurfer as a custom atlas and then subsequently used for source analysis in Brainstorm.

### 3.6 Co-registration procedure

The scalp and cortical surface envelopes were obtained from FreeSurfer and brought to Brainstorm (<http://neuroimage.usc.edu/brainstorm/>; Tadel et al., 2011). Brainstorm automatically imports surface-based anatomical atlases, and the FreeSurfer ROIs were used for co-registration. The high-resolution cortical surfaces of approximately 160,000 vertices were down-sampled to 15,000 vertices, to serve as image supports for cortically-constrained, distributed MEG source imaging (Baillet et al., 2001).

### 3.7 Data preprocessing

MEG data preprocessing and data analysis were also performed in Brainstorm, following good-practice guidelines (Gross et al., 2013). The standard steps consisted of finding and removing the artefactual contributions from heart rate and eye blinks/saccades to the MEG traces. Occurrence of eye blinks and heartbeats were detected from previously mentioned EOG and ECG electrodes in Brainstorm. Signal-space projection vectors were then calculated for each type of artefact (Uusitalo & Ilmoniemi, 1997), and the component with the highest eigenvalue was rejected for each artefact type. The data were finally down-sampled to 1000Hz.

### 3.8 MEG source reconstruction

We used the empty room noise recording to build the noise covariance matrix across MEG channels from each session. These noise statistics were used in the estimation of cortical currents with a depth-weighted L2-minimum norm approach (Baillet et al., 2001). Source analysis resulted in a linear kernel that was applied to MEG sensor data to obtain MEG source time series at each of the vertices of the subjects' cortical surface. The data were processed in Brainstorm with default depth weighting parameters (order = 0.5; maximum amount = 10).

### 3.9 Power spectrum analysis

Power spectral density (PSD) of MEG source time series was computed for all trials from 0.5 s to 4 s across all vertices (1000 ms window overlap ratio of 50%). We removed the first 500ms of each trial from our analysis to consider only the steady state portion of the visual response in the analysis (Cottetereau et al., 2011). Each PSD value was standardized to the PSD in the zero-contrast condition at the tagging frequency of interest, averaged across trials and left and right regions in every subject. A sample V1 PSD graph is shown in Figure 1C. Subsequently an offset of one was subtracted so that the response at the noise level was zero. Then, in order to normalize the data acquired in 4Hz and 6Hz bands, the power response at 6Hz was scaled so that the monocular response at 6Hz matches the monocular response at 4Hz.

### 3.10 Phase analysis

The fast Fourier transform (FFT) was used to estimate the phase of SSVER signals at each of the tagging frequencies and each vertex in the V1 ROI at 4 and 6Hz over the 0.5 s - 4 s time window, for each trial. The source location consistently responding with a maximal amplitude at both stimulation frequencies over all trials was identified and selected within V1 ROI for phase analysis. Hence only one vertex per ROI with a consistently strongest response was used for the phase analysis. We used this approach as it gave a better representation of the resultant direction for the ROI than the average or the sum of total vertices present in the ROI. The average and variance of the phase angle at the tagged frequency across trials was then calculated. Only phase measures with a variance below 0.5 rad<sup>2</sup> were kept for further analysis. In cases when the phase variability exceeded 0.5 rad<sup>2</sup>, the phase value result was not taken into consideration for finding the average between subjects' left and right V1. This conservative strategy was chosen to make sure that the delay we calculate is based on the true representation of the signal originating in each eye from our stimulation rather than the background noise. Since a variance reaching 0.5 rad<sup>2</sup> is approaching the noise level, it therefore indicates a weak inconsistent signal, the phase of which would possess no interpretable value.

The phase was always reported relative to monocular condition at maximal stimulation contrast (32%). The

group average and standard deviation were calculated across subjects in each corresponding ROI.

Phase delays were transformed into time delays measured in milliseconds: ( $[\text{angle in radians}] \times 1000 / (\text{tagging frequency} \times 2 \times \pi)$ ). Therefore, we report all phase results as a delay observed relative to the monocular stimulation condition at maximum contrast and luminance, in milliseconds.

All phase data analysis was performed using the circular statistics toolbox in Matlab ([philippberens.wordpress.com/code/circstats/](http://philippberens.wordpress.com/code/circstats/)).

#### 4. Results

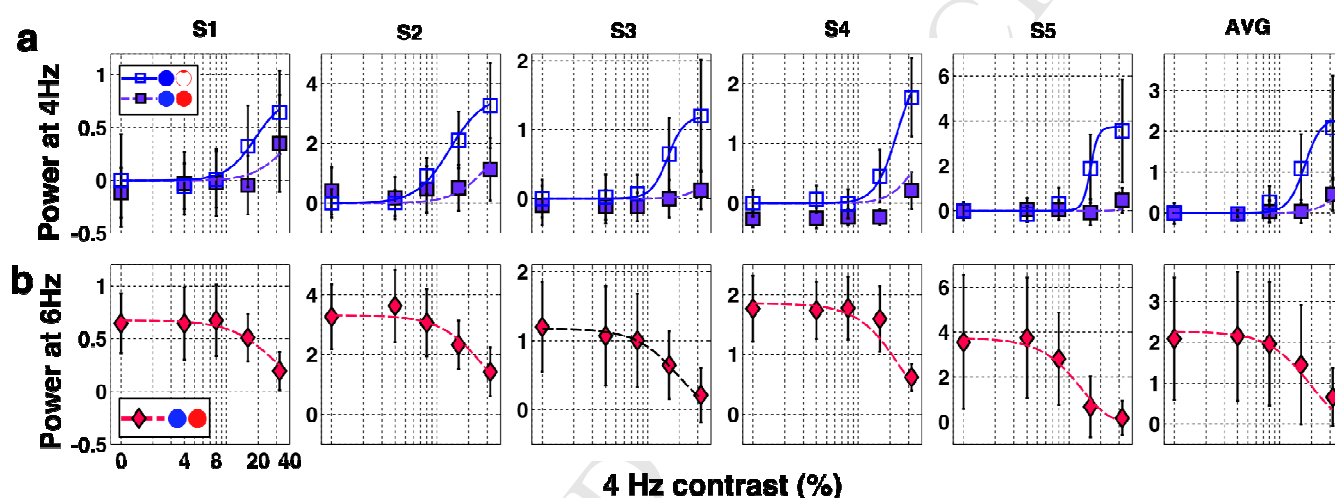


**Figure 2. Dichoptic masking.**

a. Monocular (target, blue at 4 Hz, open squares symbols) and dichoptic (masked target, purple at 4 Hz, filled squares symbols) contrast response functions for the range of contrasts (0, 4, 8, 16 and 32%) for individual participants (S1-S5) and their average (AVG) at 4Hz (target eye) in primary visual cortex.

In panels S1-S5, the error bars indicate standard deviation. Solid and dotted lines represent the normalization model for monocular and dichoptic presentations respectively. In the last panel (average), the error bars indicate the standard deviation between the subjects and the lines correspond to the model reconstruction using the average of the parameters estimated for individual subjects.

b. Dichoptic contrast response functions in the primary visual cortex responses to 32% contrast stimuli (red diamonds) presented at 6 Hz while the contrast is increased in the other eye (0, 4, 8, 16 and 32%) for individual participants (S1-S5) and their average (AVG). Dotted lines represent the interocular normalization model fits.

#### 4.1 Contrast modulation

Using the average power in V1, we built the contrast response function for monocular and dichoptic conditions (Figure 2). As the contrast of the monocular stimulus at 4Hz increased from 0 to 32%, the power of responses also increased (one-way ANOVA: main effect of target contrast;  $F=11.993$ ,  $p=0.019$ , GG corrected), responses at 16% and 32% contrast were significantly different from noise level ( $p<0.05$ ; Figure 2A). Addition of the dichoptic mask at 6Hz markedly decreased the response at 4Hz (two-way ANOVA: main effect of mask ( $F=16.539$ ,  $p=0.015$ ) and target ( $F=14.697$ ,  $p=0.013$ , GG corrected). There was a significant interaction between the masked and the monocularly presented target at 32% and 16% contrast ( $F=8.718$ ,  $p=0.032$ , GG corrected). The response to the mask presented at 6Hz and fixed at 32% contrast also showed progressive decrease as the contrast of the dichoptically presented 4-Hz stimulus was increased in the other eye (Figure 2B) (one-way ANOVA: main effect of target contrast,  $F=9.764$ ,  $p<0.001$ ).

The data obtained were fitted using a normalization model derived from the binocular combination model of Moradi and Heeger (2009). This model accounts for the way the signals from the two eyes are combined binocularly, with the activity from each eye reducing the gain for the other eye as well as for itself. Since we experimentally assigned a different frequency band to each eye, the fitting was performed independently for the two eyes contributions  $R_L$  (equation 1) and  $R_R$  (equation 2) before the combination stage. We therefore set each numerator to contain only one eye's input, whereas the denominator contained the inputs of the full normalization pool (Foley, 1994; Carandini et al., 1997; Busse et al. 2009; Reynaud et al., 2012)

$$R_L = R_{max} \frac{C_L^n}{C_{50}^n + (\sqrt{C_L^2 + C_R^2})^n} \quad (1)$$

$$R_R = R_{max} \frac{C_R^n}{C_{50}^n + (\sqrt{C_L^2 + C_R^2})^n} \quad (2)$$

$C_L$  and  $C_R$  represent the input contrasts amplitude at different temporal frequency bands seen respectively by the left and right eyes. The amplitude  $R_{max}$ , the semi-saturation constant  $C_{50}$  and the slope  $n$  are the estimated parameters. The same set of parameters was used for the two eyes inputs. The model fitted the data correctly (mean  $R^2 = 0.9703$ , Table 1), indicating that the model fully described the experimental data with as few as 3 free parameters. The continuous and dashed lines in Figure 2A and 2B show the model fit for individual subjects S1 to S5. In the rightmost panels the group average data is presented with model predictions computed from the average estimated parameters. The coefficient of determination of this prediction is still very high ( $R^2=0.9734$ ) indicating a remarkable consistency of the results between subjects.

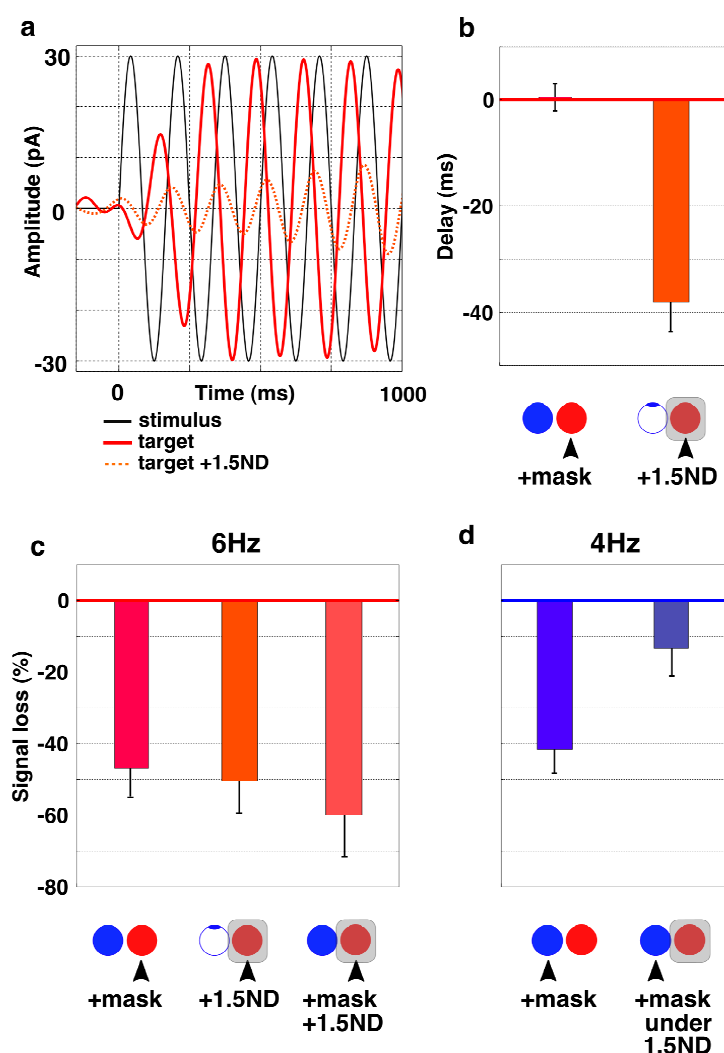


### Figure 3. Signal loss and delay in masking and under reduced luminance.

- a. V1 response as a function of time to a 6Hz monocular stimulation with (dotted line) and without (solid line) 1.5 ND filter applied, band pass filtered between 5 and 7 Hz. Black sinusoidal curve corresponds to the time course of the stimulus appearance on the screen.
- b. Delay from monocular 32% contrast condition (6Hz) computed from phase angle during dichoptic stimulation ('mask') and during monocular 1.5 ND filter application over the 6Hz stimulus ('1.5ND').
- c. Mean power loss at 6Hz compared to monocular 32% contrast condition (6Hz) during dichoptic stimulation ('mask'), during monocular 1.5 ND filter application over the 6Hz stimulus ('1.5ND') and during dichoptic stimulation while the filter was kept over the 6Hz stimulus ('mask+1.5ND').
- d. Mean power loss at 4Hz compared to monocular 32% contrast condition (4Hz) during dichoptic stimulation ('mask') at normal luminance and dichoptic stimulation while the 1.5 ND filter was kept over the 6Hz stimulus ('mask under 1.5ND'). The 1.5 ND filter over the masking eye reduced the masking effect.

## 4.2 Luminance modulation

Luminance reduction using a 1.5 ND filter was applied in both the monocular and dichoptic conditions at 32% contrast. We compared the respective effects of luminance and of contrast masking (dichoptic condition) as well as their combined effects in V1 (Figure 3).

Decreasing luminance affected the dynamics of the response by introducing delays and reducing the response amplitude and power. These changes were readily observable in band-passed (between 5 and 7Hz) filtered source traces (Figure 3A) and were quantified by computing differences between phase values (Figure 3B, see Methods) and power (Figure 3C and 3D) across conditions. Phase analysis revealed distinctly different effects of the dichoptic mask and reduced luminance conditions than those observed using signal power measures. Indeed, the presence of the dichoptic mask at 4Hz (32% contrast) did not affect the phase of the response to the 6Hz stimulus ( $T(11)=0.33$ ;  $p=0.745$ ), whereas the addition of the 1.5 ND filter produced a strong phase effect ( $T(11)=18.80$ ,  $p<0.001$ ), introducing a delay equivalent to 38ms on average. The addition of a 4-Hz dichoptic mask resulted in a 47% reduction of the 6-Hz cortical response



(Figure 3C,  $T(5) = -5.92$ ,  $p < 0.01$ ). Applying a 1.5 ND filter over the monocularly viewed stimulus resulted in a similar loss of power at 6Hz of approximately 50% ( $T(5) = -5.72$ ,  $p < 0.01$ ). The combination of the two conditions (dichoptic stimulus plus a 1.5 ND filter over the 6-Hz stimulus eye) resulted in a stronger decrease in cortical response at 6Hz of 60%, relative to the monocular response ( $T(5) = -5.28$ ,  $p < 0.01$ ).

The dichoptic condition was explored at 4Hz as well, as the notations “target” and “mask” can be used interchangeably depending upon which eye is being analyzed (Figure 3D). Adding the dichoptic mask at 6Hz resulted in a 42% signal loss compared to the response to the monocular stimulus at 4Hz ( $T(5) = -5.97$ ,  $p < 0.01$ ). When the 1.5 ND filter was applied over the 6-Hz dichoptic mask, the power restored to 13% below the monocular power value (not different from the monocular condition,  $p = 0.12$ , but different from the response power under the dichoptic mask:  $T(5) = 4.71$ ,  $p < 0.01$ ), which demonstrates the “unmasking” effect of the filter.

The finding that the signal loss observed in the reduced luminance condition (Figure 3A) was accompanied by a delay (Figure 3A) suggests the requirement of an additional temporal factor to be taken into account in models of interocular interactions. We therefore set out to incorporate this temporal aspect into a more general binocular interaction model.

### 4.3 Model Simulations

We have shown that a binocular normalization model explains the power of MEG signals in the dichoptic contrast masking experiment (Figure 2) and that reducing luminance delays the cortical processing of the stimulus. Specifically, it has been suggested that reduced luminance results in low-pass temporal filtering of the neural responses (Katsumi et al., 1986; Reynaud et al., 2013). In order to test this hypothesis, we ran simulations of the binocular combination model on temporal signals. The model parameters  $c_{50}$  and  $n$  were calibrated using the average of our previous estimates (Supplementary Table1). Monocular temporal signals at 4 and 6Hz served as inputs. These signals were filtered at the monocular stage with a gamma



probability density function that described the impulse response function (IRF) of the visual system (equation 3, Figure 6A, Robson and Troy, 1987; Boynton et al., 1996; David et al., 2006).

$$\frac{\beta^\alpha}{\Gamma(\alpha)} t^{\alpha-1} e^{-\beta t}$$

The low-pass temporal effect of the 1.5 ND filter can be reproduced empirically by increasing the value of the shape parameter  $\alpha$  of the gamma function (Figure 4A, shape and scale parameters  $\alpha$  and  $\beta$  are 2 and 20 for normal viewing, and 4 and 20 for reduced luminance; Robson and Troy, 1987; Wright et al, 2014).

Figure 4B depicts the monocular signals after passing through the first stage of monocular IRF filtering before the binocular combination step. The blue and red solid curves represent the signals at 4 and 6Hz after normal IRF filtering whereas the dotted red curve represents the 6-Hz monocular response after the low-pass IRF filtering instead. This can be compared against the solid and dotted red curves in Figure 3A, to show that the low pass IRF filtering accounts for the delay and the reduced amplitude observed in the low luminance condition.

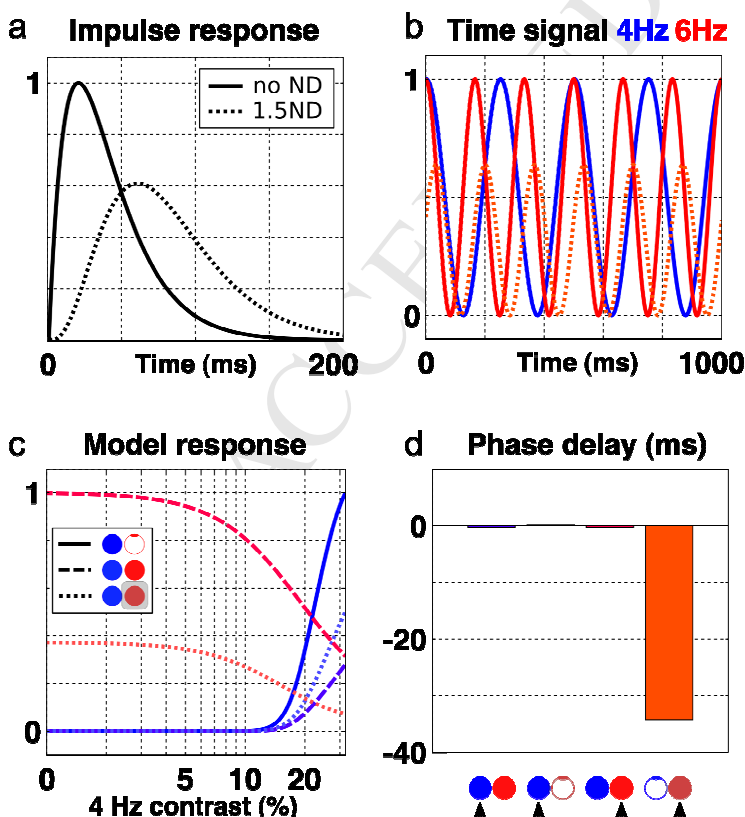


# Figure 4. Delay and phase variability in dichoptic masking and luminance reduction

- a. Impulse response functions with different shape parameters describing the filtering effect of the 1.5 ND filter.  
Shape parameter for gamma probability function is changed to approximate the temporal low pass filtering effect of the 1.5 ND filter on the visual processing. Continuous line: no filter condition: shape parameter = 2, scale parameter = 20; Dotted line: 1.5 ND filter condition: shape parameter = 4, scale parameter = 20).
- b. 4Hz (solid blue) and 6Hz (solid red) sinusoids simulating the signal obtained from the two eyes in SSVER tagging protocol through the standard filter (solid curve in a). The dotted red line represents the 6Hz signal through the low-pass filter (dotted curve in a) inducing a delay and an amplitude reduction in the signal.
- c. Response predictions at various contrast levels at normal and reduced luminance in V1 based on our model. The icons in the panel indicates five different conditions as follows:  
Solid blue: monocular response at 4Hz;  
Dashed blue: power loss due to a 6Hz dichoptic mask;  
Dashed red: response to a 6Hz mask;  
Dotted red: response to a 6Hz mask through the low-pass filter;  
Dotted blue: unmasking of a 4Hz response when the eye receiving the 6Hz signal is reduced in luminance.
- d. Predicted delay of phase in (left to right): masked condition at 4Hz, monocular viewing at 4Hz with a 1.5ND filter applied over the fellow eye, masking condition at 6 Hz and monocular reduced luminance condition at 6Hz.

We performed simulations using these time-varying signals inputs to the binocular normalization model described in equations 1 and 2. The model predictions for the power of the responses reflecting binocular interactions for normal and reduced luminance are reported in Figure 4C (compare to actual data shown in Figure 2A and 2B). The monocular response at 4Hz was predicted to increase in power as a function of contrast (solid blue line). Once a 6Hz mask is applied dichoptically at 32% contrast, a loss in power is anticipated for both the 4Hz target (dashed blue line) and the 6Hz mask itself (dashed red line). The prediction for the 6Hz mask response under the reduced luminance condition with a growing contrast in the target eye has not been fully tested experimentally (dotted red line). However, the initial point of the curve when the 6Hz mask appears at 32% contrast and a 4Hz target is at 0% contrast corresponded to our experimental findings (about 50% reduction in power compared to normal luminance condition (Figure

3C). The rest of the curve predicted a slow decay in the mask signal as a function of the target increasing in contrast. Finally, the 4Hz response was predicted to become “unmasked” when the 6Hz dichoptic mask is covered by a low-pass filter (dotted blue line). Figure 4D represents the model predictions for the temporal effect of contrast masking and luminance reduction (compare to actual data from Figure 3B). The monocular phase under the reduced luminance condition was predicted to be delayed by approximately 34ms which is comparable to the actual observation of a 38ms delay in our experimental MEG data. No delay was predicted for the binocular interaction in normal luminance.

## 5. Discussion

The interaction between left and right eye contrast signals can be described by a binocular contrast normalization process, whereby the response of each eye is divided by the combined responses of both eyes. Our work demonstrates such interaction for SSVER signals, using a frequency-tagging approach. We used signal power derived at specific temporal frequencies (those used to individually tag the left or right eye responses). Monocularly, our data demonstrates a monotonic increase in power in response to increasing contrast. These results are well in line with previous studies of responses to monocular contrast increases in EEG (Tsai et al., 2012) and MEG (Hall et al., 2005). Interestingly, Hall et al. (2005) also observed no signs of saturation of the contrast response in V1 using a different source reconstruction method (minimum norm estimate vs. the SAM beamformer by Hall et al. 2005).

Under conditions of dichoptic signal presentation, the contrast response function was shifted rightwards and significantly reduced in amplitude for signal power measures. This represents a signature of gain control, or divisive normalization (Moradi and Heeger, 2009), the purpose of which is to adjust the sensitivity of a system to keep the responses invariant. Thus, at the macroscopic levels captured in MEG, the response measured due to a change in contrast (e.g., from 32% to 16% contrast) or to the addition of the

mask in the other eye (32% contrast to both eyes) reflects the population response to relative rather than absolute contrast. Baker et al. (2015) reported only weak masking in their healthy observers (significant masking was only achieved at 26% contrast) that could potentially be explained by the lower sensitivity of EEG for measuring binocular interactions at the selected tagging frequencies (10 and 12Hz). We did not observe a shift in phase associated with the addition of the contrast mask. This is especially interesting given the similar effect both the mask and the ND filter had in the power domain.

Decrease in the luminance of interocular signals resulting from the monocular application of a 1.5 ND filter introduced a delay of 38ms and a 50% loss of power in the V1 response, compared to the monocular, non-filtered condition. ND filters alter luminance without affecting contrast. However, it could be argued that the delay we found could be due to a reduced contrast sensitivity, observed at low luminance levels (Hess 1990). This is unlikely. First, the change in contrast sensitivity would have been small, only involving high spatial frequencies within our noise stimulus (van Nes et al., 1967) and second, as previously discussed, changes in dichoptic contrast are not normally associated with changes in response phase.

The effect of an interocular imbalance in luminance stimulation is different from that of an interocular imbalance in contrast stimulation. While the effects of a luminance and contrast imbalance can both, in principle, reduce signal power, their effects in combination are sub-additive. Furthermore, the effects of a monocular reduction in luminance can mitigate against the effects of a dichoptic contrast mask (Figure 3 and Supplementary Figure 2). Importantly, dichoptic contrast masking does not produce any marked temporal change in the response, unlike a luminance imbalance, which results in a temporally delayed response (i.e. a phase delay). This could be a consequence of luminance reductions affecting signal transduction earlier in the pathway (i.e. slowing responses at the retina).

The 38ms delay we report here slightly exceeds that reported for similar ND strengths. Carkeet et al. (1997)

reported the delay introduced by various intensities of ND filters, as measured with a psychophysical of adjustment method. From their Figure 6, the delay introduced by a 1.5 ND filter varies between 15 to 30 ms between subjects. In a comparable task, Reynaud and Hess (2017) observed delays of approximately 16ms with filters of 1ND. Heravian-Shandiz et al. (1991) reported visually evoked responses to pattern stimulation being delayed by approximately 20 ms due to a filter of comparable strength (as estimated from figures). The reduction in response power associated with decreased luminance is comparable with our own data's and ranges between 30 and 50% (as estimated from Heravian-Shandiz et al., 1991). Finally, Katsumi et al. (1986) presented a range of phase and amplitude changes resulting from the application of ND filters in the range of 0 and 3ND. However, their results cannot be compared directly with ours because they applied the filters binocularly and reported only the monocular/binocular advantage. Finally, we demonstrated that reducing luminance to one eye reduces that eye's contribution to binocular processing of other signals, as can be seen by the reduced signal loss to dichoptic contrast masking in the fellow eye (compared to high percentage signal loss in normal luminance dichoptic condition). Our simulations provide a new understanding of the effects of interocular changes in luminance in terms of temporal filtering and demonstrates their importance for models of binocular signal combination in general, when the inputs from the two eyes are imbalanced.

The delay created by the reduced luminance can be appreciated from the retina all the way to the cortical level (Bieniek et al., 2013, Tobimatsu et al., 1993). Interestingly, such delays seem to occur spontaneously in conditions such as amblyopia, which has not been taken advantage of for the therapeutic use for such patients yet. The relation between the contrast attenuation and the delay, with a subsequent individual adjustment of both the parameters for the amblyopic eye in a training program is a viable therapeutic venue for the amblyopic patients. Interestingly, the reduced interocular interaction in a form of unmasking that we observe when the ND filter is placed over the 6 Hz mask, is accompanied by the delay we describe above. This unmasking effect due to the interocular delay could also serve as an explanation for the reduced interocular interaction in the amblyopic population.

In summary, using a novel steady-state MEG approach we showed how the signals from the two eyes are combined as a function of interocular luminance and contrast. We applied an interocular binocular normalization model derived from psychophysics (Ding and Sperling, 2006; Meese et al. 2006) and fMRI (Moradi and Heeger 2009) studies to describe interocular changes in contrast, showed that it can be evaluated using MEG techniques. We extended this model to account for interocular luminance changes. Overall, this work therefore provides a foundation for future research concerning how the normal pattern of binocular interactions is altered by experimental manipulations and disease states; for example, after short-term monocular deprivation (Lunghi et al., 2011; Zhou et al., 2013) and in amblyopia (Sengpiel et al., 1996, 2006), where one eye's signal totally suppresses the response of the other eye.

## 6. Acknowledgements

We would like to thank our participants for their time and efforts and Dr. Alex S. Baldwin for his helpful suggestions.

This work was supported by Natural Sciences and Engineering Research Council of Canada Discovery grant (#201603740) to RFH.

## 7. References

- Baillet, S.; Mosher, J. C. & Leahy, R. M., 2001. Electromagnetic brain mapping IEEE Signal processing magazine, *IEEE*, 18 (6) , 14-30
- Baker, D. H., Simard, M., Saint-Amour, D., & Hess, R. F., 2015. Steady-state contrast response functions provide a sensitive and objective index of amblyopic deficits. *IOVS*, 56(2), 1208-1216
- Bieniek, M. M., Frei, L. S., & Rousselet, G. A. (2013). Early ERPs to faces: aging, luminance, and individual differences. *Frontiers in psychology*, 4.
- Boynton, G. M.; Engel, S. A.; Glover, G. H. & Heeger, D. J., 1996. Linear systems analysis of functional magnetic resonance imaging in human V1. *J Neurosci*, 16 (13) , 4207-4221
- Brainard, D. H., 1997. The Psychophysics Toolbox. *Spat Vis*, 10 (4) , 433-436
- Busse, L., Wade, A. R., & Carandini, M., 2009. Representation of concurrent stimuli by population activity in visual cortex. *Neuron*, 64(6), 931-942.
- Carandini, M. & Heeger, D. J., 1994. Summation and division by neurons in primate visual cortex. *Science*,



- 540 264 (5163) , 1333-1336
- 541 Carandini, M.; Heeger, D. J. & Movshon, J. A. 1997. Linearity and normalization in simple cells of the  
542 macaque primary visual cortex. *J Neurosci*, 17 (21) , 8621-8644
- 543 Carkeet, A., Wildsoet, C. F., & Wood, J. M., 1997. Interocular temporal asynchrony (IOTA):  
544 Psychophysical measurement of interocular asymmetry of visual latency. *Ophthalmic Physiol Opt*, 17(3),  
545 255-262.
- 546 Cavanaugh, J. R.; Bair, W. & Movshon, J. A., 2002. Nature and interaction of signals from the receptive field  
547 center and surround in macaque V1 neurons. *J Neurophysiol*, 88 (5) , 2530-2546
- 548 Clavagnier, S.; Dumoulin, S. O. & Hess, R. F., 2015. Is the Cortical Deficit in Amblyopia Due to Reduced  
549 Cortical Magnification, Loss of Neural Resolution, or Neural Disorganization? *J Neurosci*, 35 (44) , 14740-  
550 14755
- 551 Cottureau, B.; Lorenceau, J.; Gramfort, A.; Clerc, M.; Thirion, B. & Baillet, S., 2011. Phase delays within  
552 visual cortex shape the response to steady-state visual stimulation. *Neuroimage*, 54 (3) , 1919-1929
- 553 David, O.; Kilner, J. M. & Friston, K. J., 2006. Mechanisms of evoked and induced responses in MEG/EEG.  
554 *Neuroimage*, 31 (4) , 1580-1591
- 555 Ding, J. & Sperling, G., 2006. A gain-control theory of binocular combination. *Proc Natl Acad Sci U S A*, 103  
556 (4) , 1141-1146
- 557 Dumoulin, S. O. & Wandell, B. A., 2008. Population receptive field estimates in human visual cortex.  
558 *Neuroimage*, 39 (2) , 647-660
- 559 Engel, S. A.; Rumelhart, D. E.; Wandell, B. A.; Lee, A. T.; Glover, G. H.; Chichilnisky, E. J. & Shadlen, M. N.,  
560 1994. fMRI of human visual cortex. *Nature*, 369 (6481) , 525
- 561 Foley, J. M., 1994. Human luminance pattern-vision mechanisms: masking experiments require a new  
562 model. *JOSA A*, 11(6), 1710-1719.
- 563 Gross, J.; Baillet, S.; Barnes, G. R.; Henson, R. N.; Hillebrand, A.; Jensen, O.; Jerbi, K.; Litvak, V.; Maess, B.;  
564 Oostenveld, R. & et al., 2013. Good practice for conducting and reporting MEG research. *NeuroImage*,  
565 Elsevier BV, 65 , 349-363
- 566 Hall, S. D.; Holliday, I. E.; Hillebrand, A.; Furlong, P. L.; Singh, K. D. & Barnes, G. R., 2005. Distinct contrast  
567 response functions in striate and extra-striate regions of visual cortex revealed with  
568 magnetoencephalography (MEG). *Clin Neurophysiol*, 116 (7) , 1716-1722
- 569 Heeger, D. J. (1991). Nonlinear model of neural responses in cat visual cortex. *Computational models of visual*  
570 *processing*, 119-133.  
571
- 572 Heravian-Shandiz, J., Douthwaite, W., & Jenkins, T., 1991. Binocular interaction with neutral density filters  
573 as measured by the visual evoked response. *Optom Vis Sci*, 68(10), 801-806.
- 574 Hess R. F. (1990). Vision at low light levels: Role of spatial, temporal and contrast filters. *Ophthalmic Physiol*  
575 *Opt*, 10, 351-359.
- 576 Katsumi, O.; Tanino, T. & Hirose, T., 1986. Objective evaluation of binocular function using the pattern  
577 reversal visual evoked response. II. Effect of mean luminosity. *Acta Ophthalmol (Copenh)*, 64 (2) , 199-205
- 578 Legge, G. E. & Foley, J. M., 1980. Contrast masking in human vision. *J Opt Soc Am*, 70 (12) , 1458-1471
- 579 Legge, G. E., 1984. Binocular contrast summation – II. Quadratic summation. *Vis Research*, (4) , 385-394
- 580 Lunghi, C.; Burr, D. C. & Morrone, C., 2011. Brief periods of monocular deprivation disrupt ocular balance

- 581 in human adult visual cortex. *Curr Biol*, 21 (14) , R538-R539
- 582 Meese, T. S.; Georgeson, M. A. & Baker, D. H., 2006. Binocular contrast vision at and above threshold. *J Vis*,  
583 6 (11) , 1224-1243
- 584 Moradi, F. & Heeger, D. J. , 2009. Inter-ocular contrast normalization in human visual cortex. *J Vis*, 9 (3) ,  
585 13.1-1322.
- 586 Norcia, A. M.; Appelbaum, L. G.; Ales, J. M.; Cottareau, B. R. & Rossion, B., 2015. The steady-state visual  
587 evoked potential in vision research: A review. *J Vis*, 15 (6) , 4
- 589 Pelli, D. G., 1997. The VideoToolbox software for visual psychophysics: transforming numbers into movies.  
590 *Spat Vis*, 10 (4) , 437-442 Busse, L.; Wade, A. R. & Carandini, M. (2009). Representation of concurrent stimuli  
591 by population activity in visual cortex. *Neuron*, 64 (6) , 931-942
- 592 Reynaud, A., Masson, G. S. & Chavane, F., 2012. Dynamics of local input normalization result from  
593 balanced short- and long-range intracortical interactions in area v1. *J Neurosci*, 32 (36) , 12558-12569
- 594 Reynaud, A., Zhou, J., & Hess, R. F., 2013. Stereopsis and mean luminance. *J Vis*, 13(11), 1-1.
- 595 Robson, J. G. & Troy, J. B., 1987. Nature of the maintained discharge of Q, X, and Y retinal ganglion cells of  
596 the cat. *JOSA A*, 4 (12) , 2301
- 597 Sengpiel, F. & Blakemore, C., 1996. The neural basis of suppression and amblyopia in strabismus. *Eye*, 10 (  
598 Pt2), 250-258
- 599 Sengpiel, F.; Jirrmann, K.-U.; Vorobyov, V. & Eysel, U. T., 2006. Strabismic suppression is mediated by  
600 inhibitory interactions in the primary visual cortex. *Cereb Cortex*, 16 (12) , 1750-1758
- 601 Tadel, F.; Baillet, S.; Mosher, J. C.; Pantazis, D. & Leahy, R. M., 2011. Brainstorm: A User-Friendly  
602 Application for MEG/EEG Analysis. *Computational Intelligence and Neuroscience*, 2011 , 1-13
- 603 Tobimatsu, S., Kurita-Tashima, S., Nakayama-Hiromatsu, M., Akazawa, K., & Kato, M. (1993). Age-related  
604 changes in pattern visual evoked potentials: differential effects of luminance, contrast and check  
605 size. *Electroencephalography and Clinical Neurophysiology/Evoked Potentials Section*, 88(1), 12-19.
- 606 Tsai, J. J.; Wade, A. R. & Norcia, A. M., 2012. Dynamics of normalization underlying masking in human  
607 visual cortex. *J Neurosci*, 32 (8) , 2783-2789
- 608 Uusital, M. A., & Ilmoniemi, R. J., 1997. Signal-space projection method for separating MEG or EEG into  
609 components. *Medical and Biological Engineering and Computing*, 35(2), 135-140.
- 610 Van Nes, F. L., Koenderink, J. J., Nas, H., & Bouman, M. A., 1967. Spatiotemporal modulation transfer in  
611 the human eye. *JOSA*, 57(9), 1082-1088.
- 612 Wright, M. C. M.; Winter, I. M.; Forster, J. J. & Bleack, S., 2014. Response to best-frequency tone bursts in  
613 the ventral cochlear nucleus is governed by ordered inter-spike interval statistics. *Hear Res*, 317 ,  
614 23-32